ISSN 0029 - 3865

CONSELHO NACIONAL DE DESENVOLVIMENTO CIENTÍFICO E TECNOLÓGICO - CNPq
CENTRO BRASILEIRO DE PESQUISAS FÍSICAS - CBPF
Coordenação de Documentação e Informação Científica - CDI
Divisão de Publicações

CBPF-NF-047/83

MOLECULAR MOTION AND CONFORMATIONAL DEFECTS IN ODD-NUMBERED PARAFFINS

by

A.F. Craievich, I. Denicolo
and J. Doucet

Rio de Janeiro
CBPF
1983

"MOLECULAR MOTION AND CONFORMATIONAL DEFECTS IN ODD-NUMBERED PARAFFINS"

A.F. Craievich[1], I. Denicolo[2], J. Doucet[3]

(1) LURE, Université Paris-Sud, Orsay, France and CNPq/CBPF -Rua Dr. Xavier Sigaud, 150 - 22290 Rio de Janeiro, RJ , Brasil

(2) Departamento de Física, Universidade Federal de Santa Catarina, 88000-Florianópolis, SC , Brasil.

(3) Laboratoire de Physique des Solides associé au CNRS, Université Paris-Sud, Bât. 510, 91405 Orsay, France.

A small angle X-ray diffraction study using synchrotron radiation of paraffins C_nH_{2n+2} with $19 \leq n \leq 27$ as a function of the temperature, allowed us to characterize the molecular disorders of the rotator phases, associated with longitudinal molecular motions and conformational defects of the molecular chains. The magnitude of these disorders increases with the molecular length in agreement with previous infrared spectroscopy results. Evidences of correlations between the concentration of conformational defects, amplitude of the longitudinal motion and orientational molecular disorder were established.

Key-words: Paraffins; Phase transitions; X-ray diffraction

INTRODUCTION

The structure of paraffins in solid state can be described by a lamellar close-packing of chain molecules with parallel long axes, which are either perpendicular or tilted with respect to the stacking plane. As the temperature increases different phase transitions were detected in most of the paraffins. The low temperature phases have a rather perfect structure (crystalline phases) and, between the crystal and the liquid, several disordered phases (rotator phases) occur.

Systematic studies of odd-numbered (1)(2)(3) and even-numbered C_nH_{2n+2} (4) with $n \leq 26$ and paraffins with $27 \leq n \leq 34$ (5) lead to a detailed characterization of the mean structure of the rotator phases. Four types of structure were found. Even paraffins with $n \leq 26$ show an hexagonal packing of the molecules. Odd-numbered paraffins with $17 \leq n \leq 21$ exhibit an R_I (orthorhombic) phase and paraffins with $n = 23$ and 25 present R_I and R_{II} (hexagonal) phases. Paraffins with $n > 26$ exhibit R_{III} (triclinic) phase or R_{IV} (monoclinic) phase, or succesively a R_{III} and a R_{IV} phase.

The rotator phases are characterized by an important molecular disorder. In the previous works the existence of orientational disorder of the molecules around their long axes was established[1]. The continuous increase of this disorder with temperature allowed us to understand the transition $R_I \rightarrow R_{II}$ in $C_{23}H_{48}$ and $C_{25}H_{52}$ as a 2nd order or weakly first order transition. The transition crystal $\rightarrow$ rotator I phase in odd-numbered paraffins with $n \leq 25$ was also explained by a drastic increase of the am-

plitude of the orientational disorder at the transition temperature [2].

Other types of molecular disorders in paraffins also received the attention of theoreticians and experimentalists by using various techniques. Small angle X-ray diffraction studies were performed to investigate the longitudinal molecular motion and intramolecular conformational defects in $C_{33}H_{68}$ (6). From infrared and Raman studies of $C_{19}H_{40}$ a spectroscopic model of the phase transition in this system was suggested (7). Other recent spectroscopic and calorimetric results, concerning odd alkanes with $17 \leq n \leq 29$, lead to a model for phase transitions based on the existence of non planar molecular conformations (8). Three specific non planar defects were identified: "end-gauche", "kink" and "double gauche"; being the main component kink defects. The concentration of non planar conformers was found to increase with chain length and temperature with a roughly linear dependence [8].

The aim of this work is to perform a systematic study by small angle X-ray diffraction of the longitudinal molecular motion and molecular conformational defects in the rotator phases of odd-numbered paraffins as function of the temperature. Paraffins C_nH_{2n+2} with $19 \leq n \leq 27$ were studied.

BASIC THEORY

The small angle X-ray diffraction technique is an useful tool to study molecular longitudinal disorder and intra-chain defects as it was shown by Strobl et al. (6). The existence and the magnitude of these disorders can be established from a set

of structural parameters related to the intensity and position of the small angle 00ℓ reflexions of powder diffraction patterns[6].

For small-angle analysis the electronic density η_c in a paraffin crystal can be considered as essentially a constant in all the volume (occupied by the molecular chain) excepted small regions between the terminal groups of the molecules which constitute layer voids.

The intensities of the Bragg reflections at small angles are only functions of the size and shape of the interface regions or layer voids. The layer voids may be characterized by the difference $\Delta\eta(z) = \eta_c - \eta(z)$, where $\eta(z)$ is the average electron density in a plane parallel to the interface, at a distance z from the center of gravity of the $\Delta\eta$ function. The integral and the second moment of $\Delta\eta(z)$ define two parameters:

$$\kappa = \int \Delta\eta(z)\, dz \qquad (1)$$

and

$$\sigma^2 = \frac{1}{\kappa} \int z^2\, \Delta\eta(z) dz \qquad (2)$$

The scattering intensities in absolute units I_ℓ of the reflections 00ℓ are associated with the structure factor B_ℓ by:

$$I_\ell = B_\ell^2 \qquad (3)$$

where B_ℓ is defined by

$$B_\ell = \int \Delta\eta(z)\, e^{2\pi i(\ell/L)z}\, dz \qquad (4)$$

being L the spacing of the layer lattice planes (see Fig. 1a). An appropriate extrapolation to the origin of the reciprocal space of the scattering intensities of the several order reflections (ℓ=1,2,3...) leads to:

$$B_\ell^2(s=0) = \kappa^2 \tag{5}$$

The parameter σ follows from:

$$\left.\frac{d^2B^2}{ds^2}\right|_{s=0} = -8\,\pi^2\kappa^2\sigma^2 \tag{6}$$

If $(\sqrt{12}\,\sigma\,\ell/L)^4 \ll 1$ for all the observed 00ℓ reflections, B_ℓ^2 have a parabolic dependence on ℓ:

$$B_\ell^2 = \kappa^2 - 4\pi^2\kappa^2\sigma^2(\ell/L)^2$$

If this condition is not fullfilled a least-square fitting of the experimental intensities, I_ℓ, to a higher degree polynomial (with even powers of ℓ), is needed to obtain κ and σ.

Three basic $\Delta\eta(z)$ functions are schematically represented in Fig. 1. Fig. 1b gives the $\Delta\eta(z)$ function for a "perfect" paraffin crystal, without rigid body longitudinal motion of the molecules and without conformational defects. The $\Delta\eta$ function can be expressed by

$$\Delta\eta(z) = \eta_c - (\varepsilon/d_s) \quad \text{if } |z| < d_s/2$$

or

$$= 0 \quad \text{if } |z| > d_s/2 \tag{7}$$

where d_s is the thickness of the void layers and ε/d_s is a correction due to the contribution to the electron density in the voids from the methyl terminal groups (6). ε is given by:

$$\varepsilon = (2/S) \cos \psi$$

where S is the cross-section per chain and ψ the tilting angle of the molecule.

The thickness d_s can be estimated using the spacing L and the molecular length L_k along which the electronic density is constant and equal to η_c. We then have:

$$d_s = L - L_k \cos \psi \qquad (8)$$

From the geometry of the molecule it is easy to check that L_k is equal to (n - 1) x 1.273 Å plus a small contribution of the terminal methyls which is of the order of 1.2 Å leading to $L_k \simeq (n \times 1.273)$Å as it has been assumed in reference (6).

The long lattice spacings L are approximately constant within the domain of stability of the crystal and rotator phases of each paraffin, but a discontinuity is observed at the transition temperature. The spacing of the rotator phase, L(R), is slightly higher than that of the crystal phase L (C).

In order to obtain the parameter d_s of the rotator phase, we assume an homogeneous dilatation of the system. This assumption leads to $L_k(R)$ value (rotator phase) which can be obtained from $L_k(C)$ of the crystal phase by $L_k(R) = [L(R)/L(C)]L_k(C)$. Thus the $d_s(R)$ parameters can also be determined from equation 8.

An alternative assumption is the invariance of the chain length at the phase transition. In this case $d_s(R) = L(R) - L_k$, where

$L_k = n \times 1.273$ Å. This assumption implies that the increase in L at the phase transition reflects only an increase in d_s.

The average local thickness d_{av} of the layer is obtained from equations 1 and 7. They lead to:

$$d_{av} = (\kappa + \varepsilon)/\eta_c \qquad (9)$$

For a perfect crystal (rectangular shaped profile):

$$d_{av} = d_s \qquad (10)$$

and the relationship between d_s and σ can be determined from equation 2:

$$\sigma^2 = d_s^2/12 \quad \text{or} \quad D_t = \sqrt{12}\,\sigma = d_s \qquad (11)$$

A schematic profile of an imperfect paraffin crystal with exclusively longitudinal "rigid body" motion is shown in Fig. 1c. Its main features are:

$$d_{av} = d_s \quad \text{and} \quad d_{av} < D_t \qquad (12)$$

In the crystal with intrachain defects (schematically shown in Fig. 1d) there is an effective shortenning of the molecules, leading to

$$d_s < d_{av} \quad \text{and} \quad d_{av} < D_t \qquad (13)$$

The difference $\Delta Y = d_{av} - d_s$ allows to estimate the concentration of intrachain defects (6).

Assuming the validity of equation 10 for the crystalline phase of each paraffin, it is possible to determine κ and σ (and consequently d_{av} and D_t) for all the phases of every paraffin from intensities I'_ℓ obtained in relative scale. We have in this case, instead of equation 3, the following expression:

$$B_\ell^2 = C\ I'_\ell \qquad (14)$$

where C is a proportionality factor which depends on the particular experimental conditions. Assuming $d_s = d_{av}$ for the crystalline phase, equations 1,5,8 and 9 lead to

$$C = \frac{[(L-L_k\ \cos\psi)\eta_c - \varepsilon]^2}{I'_\ell\ (0)} \qquad (15)$$

where L, L_k, ψ, η_c and ε are known parameters and I'_ℓ (0) is the extrapolated intensity to s=0, in relative units, at a temperature corresponding to the crystalline phase. For a given compound the factor C is independent of temperature.

SAMPLES AND EXPERIMENTAL METHOD

The samples used in this work were purchased from Fluka, with the following purity grade: $C_{19}H_{40} > 99\%$, $C_{21}H_{44} > 97\%$, $C_{23}H_{48} > 99\%$, $C_{25}H_{52} > 98\%$, $C_{27}H_{56} > 98\%$. No further purification was performed.

The small X-ray diffraction experiments were carried out on powder samples using the synchrotron radiation facility at LURE. The beam was monochromatized ($\lambda = 1.608$ Å) and focussed by means of a elastically bent germanium crystal. The beam had a point-like cross-section and its intensity was continually

RESULTS AND DISCUSSION

monitored by means of an ionization chamber. The powder samples were held at constant temperature during the data collection in a specially designed water-heated cell. The X-ray diffraction diagrams were recorded by means of a Elphyse position sensitive detector. Typical counting times were about 200 s.

The integrated intensity of each reflection, on a relative scale, was determined by substracting the background from the total profile. They were corrected by the Lorentz factor and normalised to a constant intensity of the incident X-ray beam.

RESULTS AND DISCUSSION

Two of the experimental X-ray diagrams of $C_{21}H_{44}$ at different temperatures are given in Fig. 2. The evident differences between the diagrams are an increase in intensity of the lowest order reflection in the rotator phase and a more rapid diminution of the intensity of high order reflections. These general features, in every studied paraffin, mean that the transitions crystalline → rotator phases are accompannied by important increases of κ and σ (eq. 5 and 6).

Small angle X-ray diffraction diagrams of all the analysed paraffins were obtained in equivalent conditions at different temperatures. The κ and σ parameters were obtained from the slope and the extrapolated value at $s = 0$ of a fourth degree polynomial for the structure factor.

$$B_\ell^2 = A_o + A_2\, \ell^2 + A_4\, \ell^4$$

The coefficients A_0, A_2 and A_4 have been determined by least-square fitting of the intensities of the 00ℓ Bragg peaks. The experimental X-ray intensities were previously corrected for the Lorentz factor and put in absolute units by means of equation 15. Two of these fittings are shown in Fig. 3 for one of the studied paraffins. Previous studies on these systems[1][2][3] furnished us the different parameters: L (long lattice spacing), L_k (length of the extended molecule along which the electronic density is equal to η_c), ψ(tilting angle), S(chain cross-section) and ε(terminal methyl correction), which were needed to calculate d_s, d_{av} and D_t of every paraffin. These parameters are listed in Table I.

The experimental temperature dependences of d_{av} and D_t are plotted in Fig. 4 for every studied paraffin. The major feature related to the d_{av} parameters is their sharp increase at the transition temperatures. The value d_{av} (which is assumed equal to d_s in the crystalline phase) remains approximately constant and higher than d_s within the temperature domain of stability of the rotator phase.

The approximate constancy of d_{av} in the rotator phases (Fig. 4) indicates that the conformational molecular defects are mainly formed at the transition crystal → rotator. No further significant formation of intramolecular defects occurs at increasing temperatures.

The temperature dependence of D_t for every paraffin within the rotator temperature domain, is also shown in Fig. 4. The D_t parameter for the crystalline phase is not plotted in Fig. 4 because of its poor accuracy. The small decay of B_ℓ^2 for increasing ℓ in the crystalline phases leads to the calculation of differences between large similar quantities and, consequently, to large error bars. The plots of D_t show clear increases as functions of both temperature and molecular length. The estimated errors in D_t decrease from 4% for C_{19} to 2% for C_{27}.

In order to bring into closer scrutiny the dependences of d_s, d_{av} and D_t on the molecular length, we have plotted in Fig. 5 their average values in the temperature domain of stability of the rotator phase. The inequality $d_s < d_{av}$, which holds for every paraffin, is an expected feature for systems containing conformational molecular defects (equation 13). The large difference between D_t and d_{av} ($d_{av} \ll D_t$) can be mainly attributed to the molecular motions, the effect of which is to increase D_t.

A rough estimate of the defect concentration in paraffins with non tilted molecules, is given by the quotient between $\Delta Y = d_{av} - d_s$ and the molecular shortening per kink. In case of paraffins with tilted molecules (e.g. $C_{27}H_{56}$) ΔY must be previously divided by $\cos\psi$ in order to determine the over all shortening along the long molecule axes. In the rotator phase the dependence on n of d_{av}, plotted in Fig. 5, shows a linear increase. The parameter d_s remains approximately constant. By assuming a molecular shortening of about 1.3 Å per kink, the experimental difference ΔY plotted in Fig. 6, indicates a concentration of molecules with kink defects which increases with n.

The lower curves of Fig. 6 with the scale at right gives the fraction of molecules with kink defects ($C_M = \Delta Y/1.3$ Å). The linear dependence in Fig. 6 can be expressed by

$$C_M = 0.037(n - n_o) \qquad (16)$$

where n_o corresponds to the minimum chain length for the existence of a kink. Equation 16 implies that, for a very long chain length, the fraction of kinks per CH_2 site would became constant and equal to 3.7%. Under our assumption of homogeneous dilatation at the phase transition the minimum chain length necessary for the existence of a kink

is equal to 11. The alternative assumption of invariant chain length leads to a higher parameter d_s ($d_s \simeq 2.30$ Å). This yields a value of $n_o \simeq 19$.

The parameters D_t also show sharp increases at the transition temperatures. These parameters are equal to about 2Å in the crystal phases and reach, above the transition temperature, average values ranging form 3.8Å for C_{19} to 7.1Å for C_{27} (Fig. 4). Being $D_t >> d_{av}$ for every paraffin, we conclude that the main contribution to D_t in rotator phases is due to the "rigid body" longitudinal motion of the molecules.

The relationship between the interlayer void profile function $\Delta\eta(z)$ and the distribution function f(z) for the molecular positions, in systems with only longitudinal molecular motion, is given by the convolution:

$$\Delta\eta(z) = f(z) * \Delta\eta_o(z) \qquad (17)$$

where $\Delta\eta_o(z)$ is the electronic density function associated to the crystal without longitudinal molecular displacements. A rough estimate of the mean square displacement root, ΔZ, of the molecular displacements has been obtained by assuming a step function for $\Delta\eta_o(z)$ and a gaussian function for the distribution f(z). Equation 16 has been numerically solved to obtain the dependence between ΔZ and the equivalent parameter σ (or D_t) of the layer-void profile function $\Delta\eta(z)$

In addition to the function ΔY, Fig. 6 gives the estimated values of the mean molecular displacement square root ΔZ as a function of the molecular length. The linear dependences on n of ΔZ and ΔY, which are apparent in Fig. 6, suggest a correlation

between the molecular shortening (due to kink defects) and the longitudinal molecular motion. We explain this correlation as due to the enhancement of the longitudinal molecular displacement, which is produced by the the formation of local voids at the ends of the molecules with defects.

The continuous increase of the molecular displacement (associated with the increase of D_t) with temperature within the stability domain of the rotator phases (Fig.4), seems to be correlated with the temperature variation of the quotient between the two short lattice parameters (2). The approaching of the orthorhombic phase structure towards an hexagonal structure at rising temperature is accompanied by an continuous increase of orientational disorder (2) and a consequent decrease of lateral molecular interaction. These progressive loosening of lateral interaction may contribute to the observed important increase of longitudinal molecular motion.

The expected related effect of loosening of the lateral molecular interaction in the rotator II (hexagonal) phase, would be a lower variation of D_t and ΔZ with temperature. This effect is not apparent in our experimental results since no evidence for the phase transition $R_I \rightarrow R_{II}$ was found in the plots of Fig. 4.

CONCLUSIONS

In addition to the previously reported orientational disorder, the rotator phases of odd-numbered paraffins with $19 \leq n \leq 27$ exhibit clear evidences of intramolecular conformational defects and longitudinal molecular motion.

The main features of these structural disorders, which were infered from our small-angle X-ray diffraction results, are:

a) The molecular conformational defects are mainly formed (or exclusively) at the transition crystal → rotator I temperature.

b) The concentration of intramolecular defects is a linear function of the molecular length.

C) A minimum chain length is necessary for the existence of a kink

d) The longitudinal molecular motion greatly increases at the transition crystal → rotator I temperature.

e) The amplitude of the longitudinal molecular motion is higher in paraffins having longer molecules.

f) The amplitude of the longitudinal molecular displacements and the defect concentration (described in items d and e) are correlated.

g) The amplitude of the longitudinal motion increases with temperature within the stability domain of the rotator phases and shows a qualitative correlation with the continuous increase of the previously reported[2][3] orientational disorder.

The conclusion b implies that the number of defects per CH_2 group would became constant for very long molecules. The deduced value of n_o, related to the minimum chain length necessary to provide mechanical stability for the kink, depends on the assumptions about the discontinuous variation of the long spacing L at the phase transition. The lower value ($n_o = 11$) corresponding to the assumption of homogeneous dilatation is consistent with modelling calculations done on kinks. However the higher value ($n_o = 19$) agrees with the conclusion of Zerbi et al. (7) on the absence of kink defects for shorter chains. The minimum chain length for the existence of kinks deduced by Maroncelli et al. (8) in their spectroscopic work ($n_o \simeq 15$) lies between the two values obtained from our experimental results.

The present results support the idea outlined in ref. 5 which relates the increase of disorder in paraffins with increasing length, with the different nature of the structures of the rotator phases in paraffins with n higher and lower than 26. The amplitude of the longitudinal motion and the high concentration of kink defects in $C_{27}H_{56}$ induces changes in the "mean" molecular symmetry which may be significant enough to eliminate the mirror plane perpendicular to the long axis. The lower molecular symmetry allows the tilting of the molecule and the structure of the rotator phases, which are orthorhombic or hexagonal for $n \leq 26$, becomes triclinic or monoclinic for $n > 26$.

These results also support incoherent quasi elastic neutron scattering experiments, performed on these same compounds[9], from which the existence of molecular distortions, longitudinal motions and an increasing disorder with, both, increasing molecular length and temperature have been infered.

The correlation between the molecular orientational disorder, longitudinal motion and intramolecular defects is clearly evident from these experimental results. To bring into closer scrutiny this correlated behaviour, further experimental work in even-numbered paraffins and binary systems is in progress.

REFERENCES

1) J. Doucet, I. Denicolo, A. Craievich, J. Chem. Phys. 75, 1523 (1981).

2) J. Doucet, I. Denicolo, A. Craievich, A. Collet, J. Chem.Phys. 75, 5125 (1981).

3) G. Ungar, J. Chem. Phys. 87, 689 (1983).

4) I. Denicolo, J. Doucet, A. Craievich, J. Chem. Phys. 78, 1465 (1983).

5) J. Doucet, I. Denicolo, A. Craievich, C. Germain, to be published (1983).

6) G. Strobl, B. Ewen, E.W. Fischer, W. Presezek, J. Chem. Phys. 61, 5257 (1974).

7) G. Zerbi, R. Magni, M. Gussoni, K.H. Moritz, A. Bigotto, S. Dirlikov, J. Chem. Phys. 75, 3175 (1981).

8) M. Maroncelli, S.P. Qi, H.L. Strauss, R.G. Snyder, J. Amer. Chem. Soc. 104, 6237 (1982).

9) J. Doucet, A.J. Dianoux, to be published.

FIGURE CAPTIONS

Fig. 1 - Schematic $\eta(z)$ function for perfect crystals (a). Schematic $\Delta\eta(z)$ functions for (b) perfect crystals, (c) crystals with, only "rigid body" longitudinal molecular motion and (d) crystals containing molecules with conformational defects.

Fig. 2 - Experimental small-angle X-ray diffraction diagrams of an odd-numbered paraffin ($C_{21}H_{44}$) below and above the crystal (C)-rotator (R) transition temperature. One of the curves was horizontally displaced for clarity.

Fig. 3 - Plots of the square of the structure factors deduced from X-ray diagrams of $C_{21}H_{44}$. The continuous lines are the fourth order polynomial obtained by least square fitting.

Fig. 4 - Temperature dependence of d_{av} and D_t for odd-numbered paraffins with different molecular length. D_t is only given within the temperature domain of stability of the rotator phase.

Fig. 5 - Upper plot: Dependence of the average value of the D_t parameter of the rotator phase. The bars indicate the minimal and maximal D_t within the rotator phases of each paraffin. Lower plots: average values of d_{av} and d_s in the rotator phase (n indicates the number of carbon atoms in each molecule).

Fig. 6 - Full circles: Average values within the rotator phases of the mean displacement square root ΔZ, associated to the longitudinal motion of the molecules. Empty circles: this plot gives with the left scale the average shortening of the molecules due to kinks and with the right scale the fraction, C_M, of molecules with kinks.

Table 1 - Structural parameters: L(long layer spacing), L_k(molecular length), ψ(tilting angle), S(cross-section area per chain) and ε(terminal methyl correction) (1)(2)(5).

Table I

n	$L[\mathring{A}]$ C - R	$L_k[\mathring{A}]$	ψ[deg] C - R	$S[\mathring{A}]$ C - R	$\varepsilon[e\mathring{A}^{-2}]$ C - R
19	26.15 - 26.35	24.19	0	18.60 - 19.60	0.108 - 0.102
21	28.65 - 28.92	26.73	0	18.67 - 19.60	0.107 - 0.102
23	31.20 - 31.61	29.28	0	18.68 - 19.70	0.107 - 0.102
25	33.70 - 34.27	31.82	0	18.52 - 19.70	0.108 - 0.102
27	36.43 - 36.50	34.37	0-11	18.80 - 19.80	0.106 - 0.099

Table 1 - Structural parameters: L(long layer spacing), L_k(molecular length), ψ(tilting angle), S(cross-section area per chain) and ε(terminal methyl correction) (1)(2)(5).

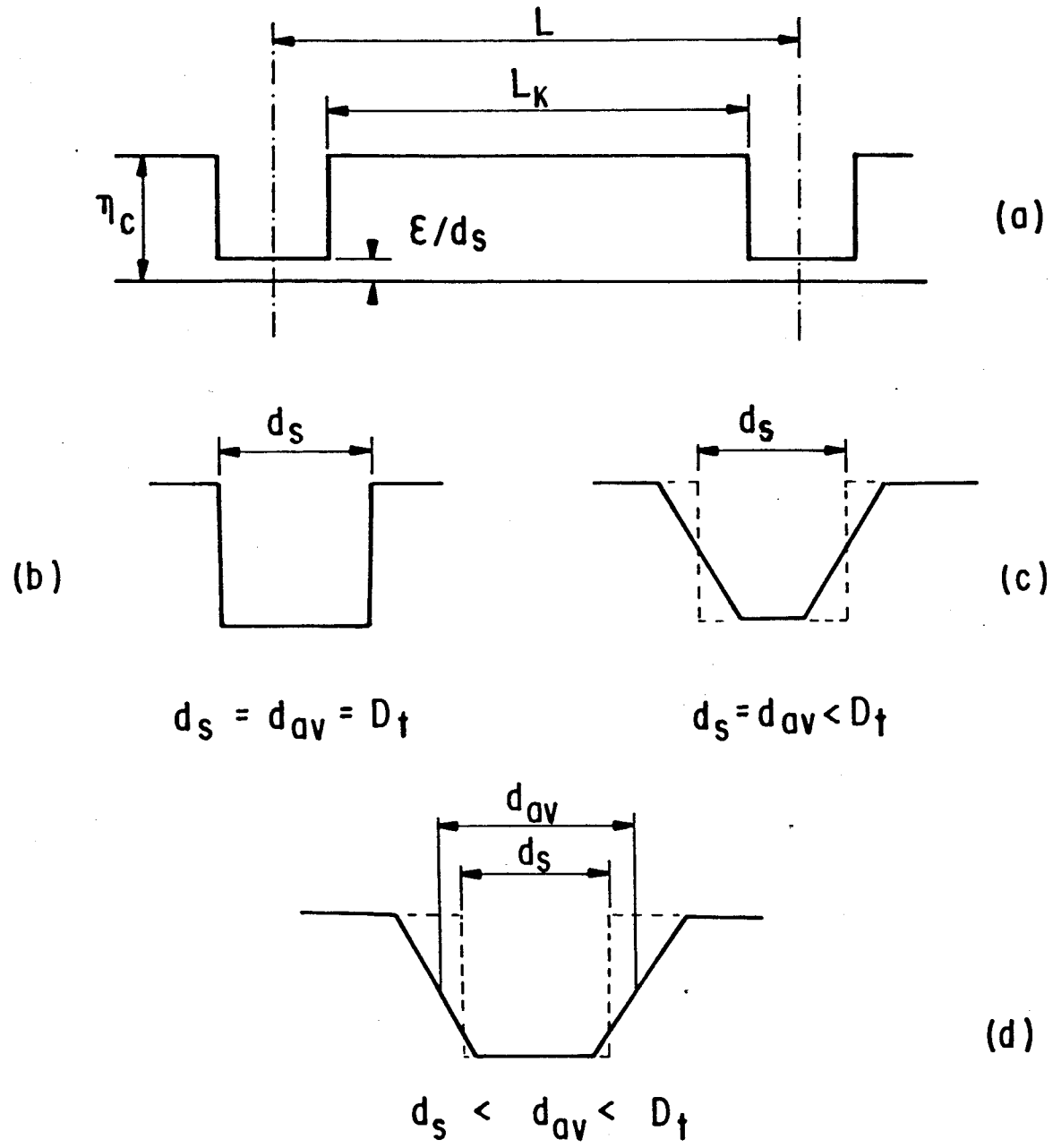
L
L_K
η_c
ε/d_s
(a)
d_s
(b)
d_s
(c)
$d_s = d_{av} = D_t$
$d_s = d_{av} < D_t$
d_{av}
d_s
(d)
$d_s < d_{av} < D_t$

FIG. 1

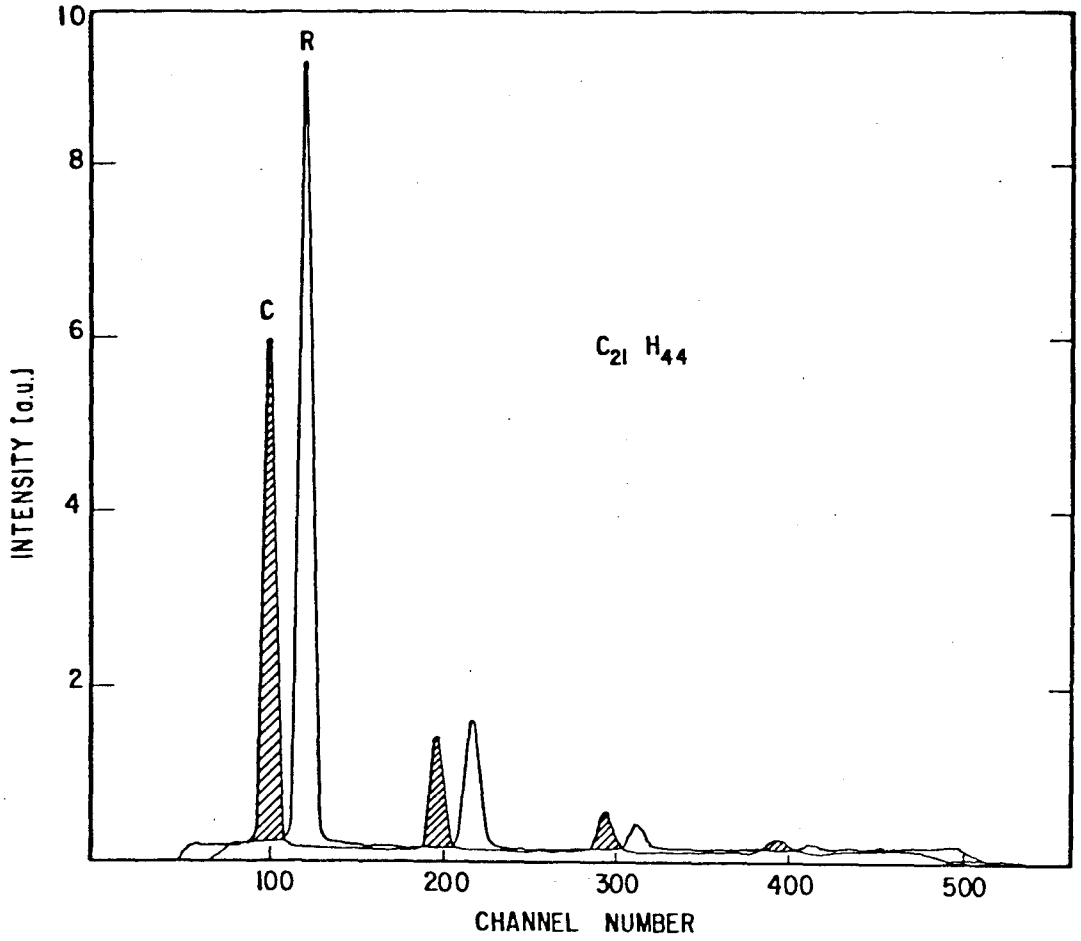
10
8
6
4
2
INTENSITY (a.u.)
R
C
C_{21} H_{44}
100
200
300
400
500
CHANNEL NUMBER

FIG. 2

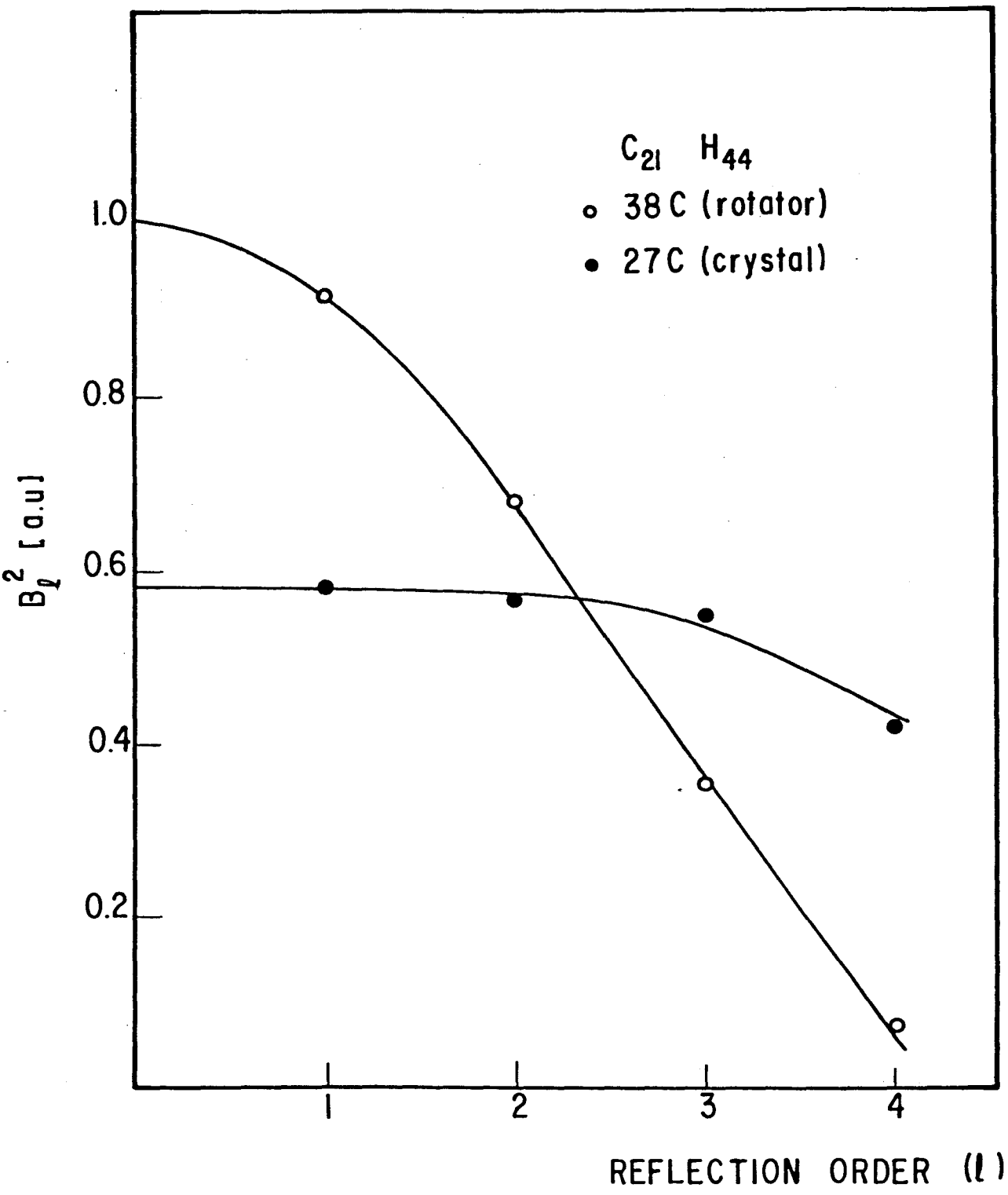
C_{21} H_{44}
o 38 C (rotator)
• 27 C (crystal)
1.0
0.8
0.6
0.4
0.2
B_l^2 [a.u]
1
2
3
4
REFLECTION ORDER (l)

FIG. 3

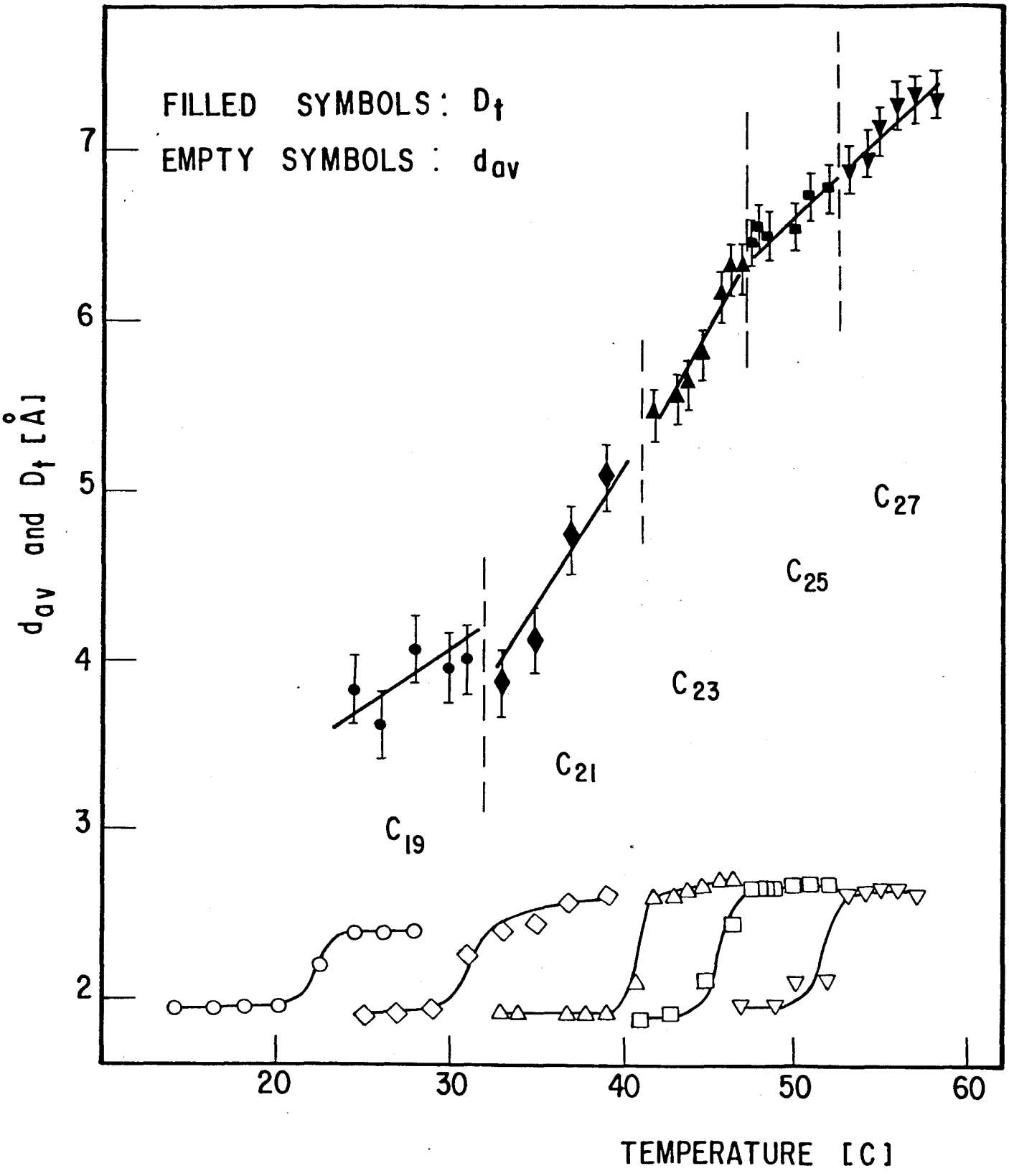
FILLED SYMBOLS : D_t
EMPTY SYMBOLS : d_{av}
d_{av} and D_t [Å]
7
6
5
4
3
2
20
30
40
50
60
TEMPERATURE [C]
C_{19}
C_{21}
C_{23}
C_{25}
C_{27}

FIG. 4

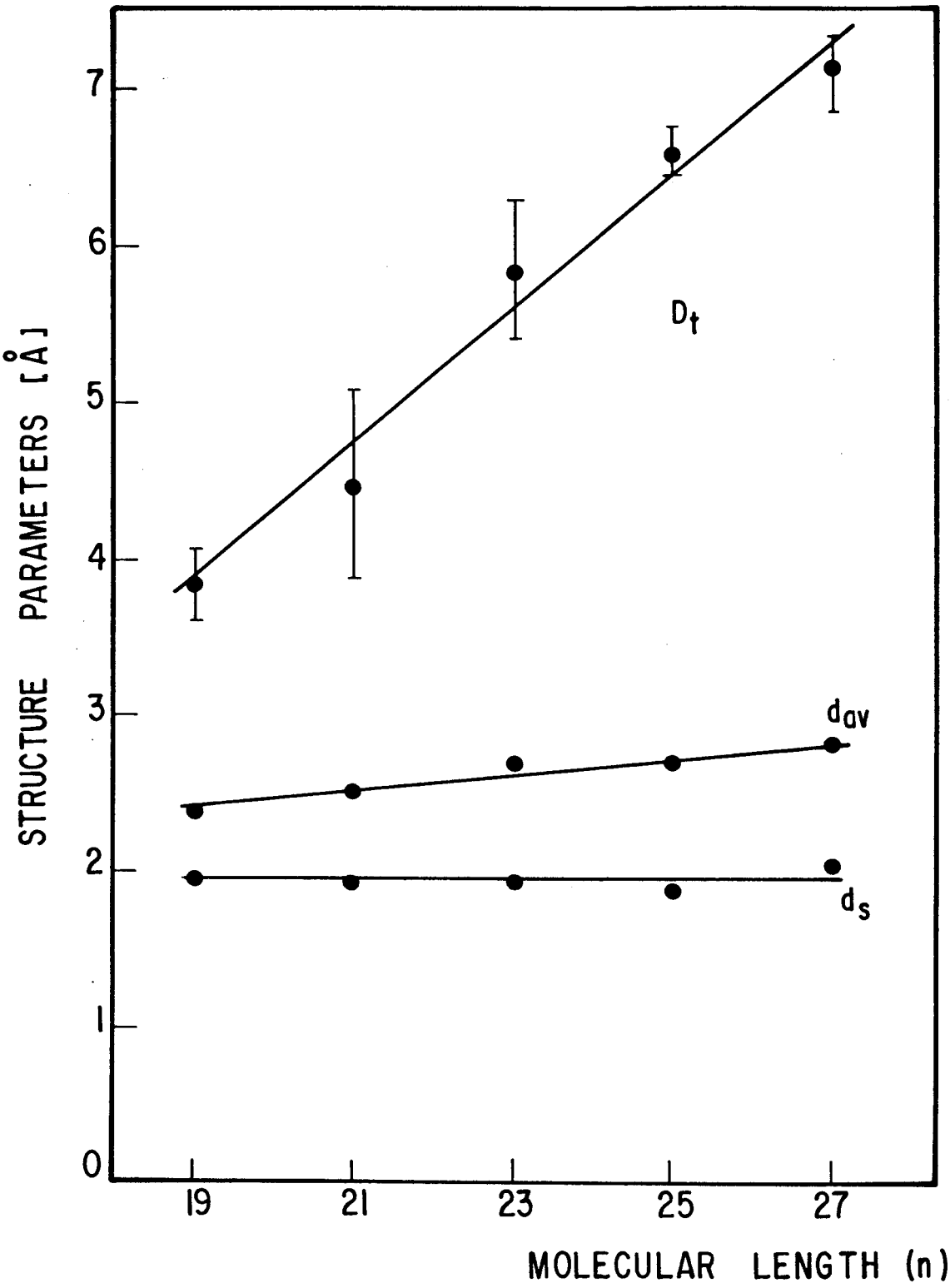
STRUCTURE PARAMETERS [Å]
0
1
2
3
4
5
6
7
19
21
23
25
27
MOLECULAR LENGTH (n)
D_t
d_{av}
d_s

FIG.5

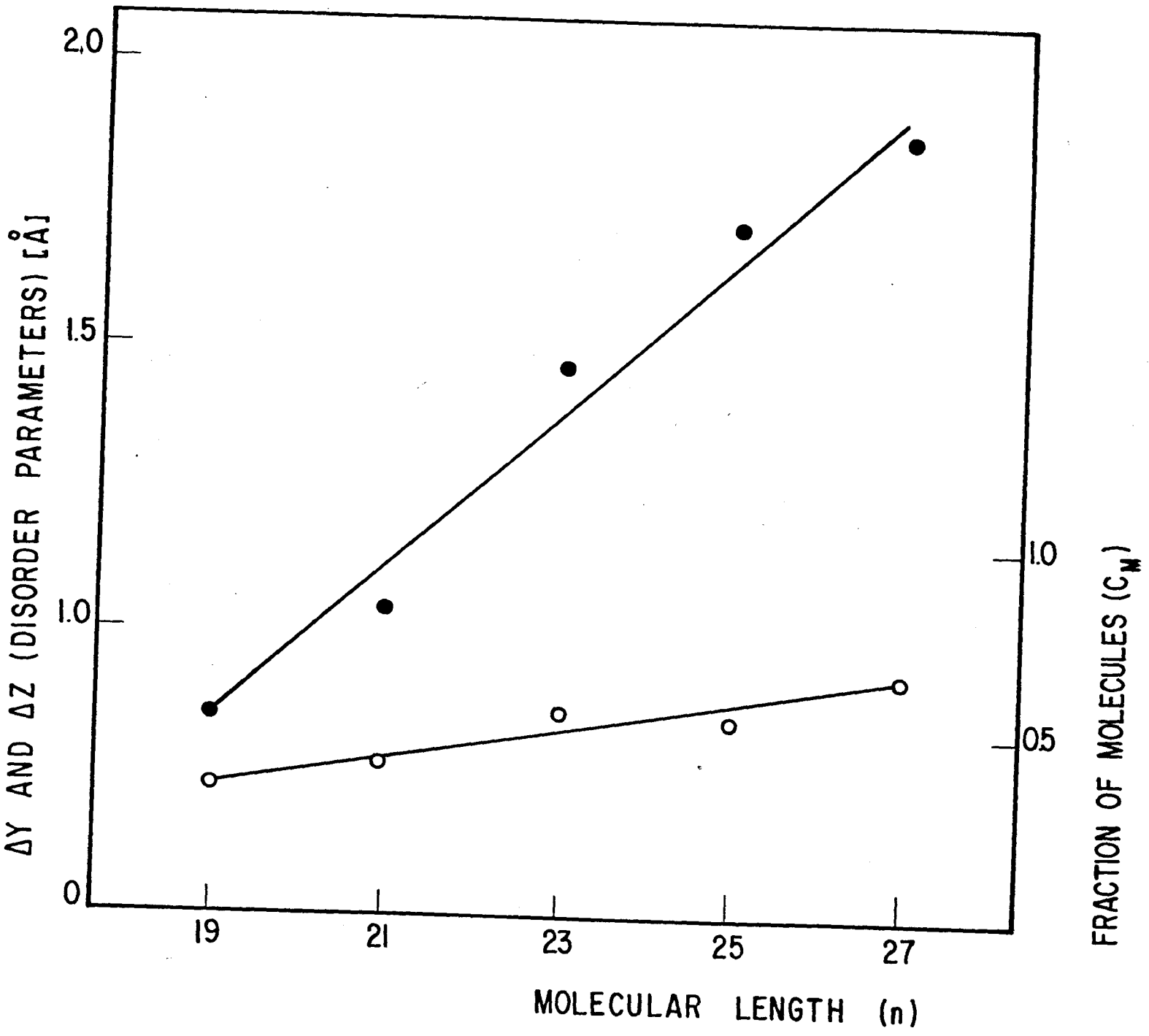
2.0
1.5
1.0
0
ΔY AND ΔZ (DISORDER PARAMETERS) [Å]
1.0
.5
FRACTION OF MOLECULES (C_M)
19
21
23
25
27
MOLECULAR LENGTH (n)

FIG. 6